Adaptive Energy Control of Longitudinal Aircraft Dynamics

Ashwin Anandakumar* and Dennis S. Bernstein †
Department of Aerospace Engineering, University of Michigan, Ann Arbor, MI 48109.

Ankit Goel‡
Department of Mechanical Engineering, University of Maryland, Baltimore County, MD 21250.

The Total Energy Control System (TECS) is a method to control airplane longitudinal flight dynamics by regulating energy and energy balance. This multiple input, multiple output method accounts for the highly coupled nature of aircraft dynamics and allows for control of airspeed and altitude with a proportional-integral controller. This paper reviews the heuristic TECS control law and then validates it in a MATLAB simulation. Next, an adaptive TECS is designed by augmenting the fixed-gain controllers in a nominal TECS with retrospective cost optimization-based adaptive controllers. It is shown through simulations that adaptive augmentation improves the closed-loop performance and accelerates the tuning process.

I. Nomenclature

L	=	Lift
D	=	Drag
M	=	Moment relative to the center of mass
T	=	Thrust applied by the engine
V	=	Speed of the aircraft
h	=	Altitude
γ	=	Flight-path angle
θ	=	Pitch angle
α	=	Angle-of-attack
δ_{e}	=	Elevator-deflection angle

II. Introduction

In the longitudinal dynamics of an aircraft, the speed and the altitude are deeply coupled. Regulating the speed and altitude simultaneously is thus a challenging problem. Intuitively, thrust affects the speed and elevator angle affects the flight-path angle, and thus the altitude. However, if only the thrust is increased while keeping the elevator angle constant, the increased lift will cause the altitude to increase, and thus elevator angle must be changed to maintain the altitude. On the other hand, if the elevator angle is changed to increase the altitude, the change in lift and drag will cause the aircraft to slow down, and thus the thrust must be increased to maintain the speed. Various approaches to independently regulate the speed and the altitude of an aircraft are described in [1].

The total energy control system (TECS) proposed in [2]–[4] regulates the speed and the altitude of an aircraft by affecting the total energy and the energy distribution. TECS has been widely applied to a variety of platforms [5], [6]. Several extensions of TECS have been developed in [6]–[9]. However, in all cases, TECS has to be heuristically tuned.

This paper develops an adaptive flight control system which consists of a nominally tuned total energy control system and an adaptive controller updated by retrospective cost optimization to automate and accelerate the tuning of TECS. The retrospective cost optimization based adaptive control has previously been applied to develop an adaptive autopilot for multicopters [10], [11], adaptive flight control system [12], [13], and active noise control system [14]. The main contribution of this paper is the development of the adaptive TECS and numerical investigation of potential performance improvements.

*Undergraduate Student, Department of Aerospace Engineering, University of Michigan, Ann Arbor, MI 48109.
†Professor, Department of Aerospace Engineering, University of Michigan, Ann Arbor, MI 48109..
‡Assistant Professor, Department of Mechanical Engineering, University of Maryland, Baltimore County, MD 21250.

The paper is organized as follows. Section III describes the longitudinal aircraft dynamics model used to simulate the dynamics in this paper, Section IV briefly reviews the total energy control system proposed in [2], Section V presents the adaptive total energy control system, Section VI reviews the retrospective cost adaptive control algorithm, and Section VII presents the simulation results of both the TECS and the adaptive TECS. Finally, the paper concludes in Section VIII with a summary of results in the paper.

III. Longitudinal Aircraft Dynamics

This section derives the equations of motion of the longitudinal dynamics for an aircraft using the coordinate-free approach.

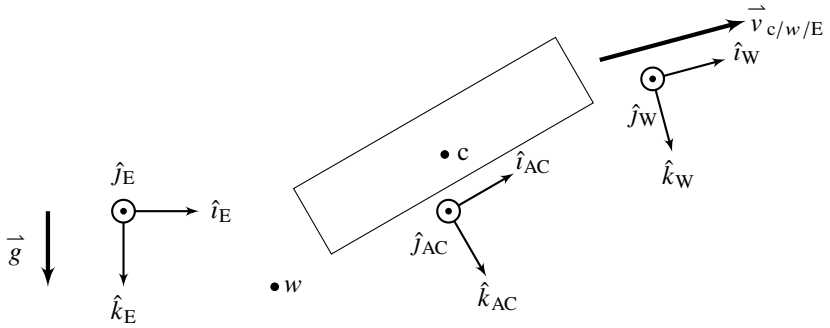

Fig. 1 Frames used to derive the equations of longitudinal motion of an aircraft.

Let $\mathrm{F_E}$ be a frame fixed to the Earth such that $\hat{k}_E$ is aligned with gravity and the fuselage lies in the $\hat{\imath}_E - \hat{\jmath}_E$ plane. Let $\mathrm{F_{AC}}$ be a frame attached to the aircraft such that $\hat{\imath}_{AC}$ is along the fuselage, $\hat{\jmath}_{AC}$ is along the wing, and $\hat{k}_{AC}$ points downwards. The frames $\mathrm{F_E}$ and $\mathrm{F_{AC}}$ thus satisfy

$$\mathrm{F_E} \xrightarrow[2]{\theta} \mathrm{F_{AC}}. \tag{1}$$

Let c denote the center of mass of the Aircraft. The velocity of c relative to w with respect to $\mathrm{F_E}$ is denoted by $\vec{v}_{c/w/E}$, where w is a fixed point on Earth and is assumed to have zero inertial acceleration. Let $\mathrm{F_W}$ be a frame such that $\hat{\imath}_W = \hat{v}_{c/w/E}$ and $\hat{\jmath}_W = \hat{\jmath}_{AC}$. The frames $\mathrm{F_E}$ and $\mathrm{F_W}$ thus satisfy

$$\mathrm{F_E} \xrightarrow[2]{\gamma} \mathrm{F_W}, \tag{2}$$

where γ is the flight-path angle. Finally, it follows from (1) and (2) that the angle of attack α satisfies

$$\alpha \triangleq \theta - \gamma, \tag{3}$$

and frames $\mathrm{F_{AC}}$ and $\mathrm{F_W}$ thus satisfy

$$\mathrm{F_W} \xrightarrow[2]{\alpha} \mathrm{F_{AC}}. \tag{4}$$

Note that $\vec{v}_{c/w/E} = V\hat{\imath}_W$.

Next, the total force on the aircraft is

$$\vec{f}_{AC} = mg\hat{k}_E - L\hat{k}_W - D\hat{\imath}_W + T\hat{\imath}_{AC}. \tag{5}$$

and the total moment relative to c is

$$\vec{M}_{AC/c} = M\hat{\jmath}_E, \tag{6}$$

where m is the mass of the aircraft and the total lift L, total drag D, thrust T, and total moment M are parameterized by

$$L = \frac{1}{2}\rho S V^2 C_{\mathrm{L}}, \tag{7}$$

$$D = \frac{1}{2}\rho S V^2 C_{\mathrm{D}}, \tag{8}$$

$$M = \frac{1}{2}\rho S V^2 C_{\mathrm{M}} \bar{c}, \tag{9}$$

and $\bar{c}$ is the chord length. The lift, drag, and moment coefficients C_{L}, C_{D}, and C_{M} are parameterized by

$$C_{\mathrm{L}} = C_{\mathrm{L}_0} + C_{\mathrm{L}_\alpha}\alpha + C_{\mathrm{L}_{\delta_{\mathrm{e}}}}\delta_{\mathrm{e}}, \tag{10}$$

$$C_{\mathrm{D}} = C_{\mathrm{D}_0} + C_{\mathrm{D}_\alpha}\alpha, \tag{11}$$

$$C_{\mathrm{M}} = C_{\mathrm{M}_0} + C_{\mathrm{M}_\alpha}\alpha + C_{\mathrm{M}_{\delta_{\mathrm{e}}}}\delta_{\mathrm{e}}, \tag{12}$$

where δ_{e} is the elevator deflection and the other coefficients are assumed to be available from experiments. The various coefficients used in this paper are given in [15].

Resolving the force $\vec{f}_{\mathrm{AC}}$ and the inertial acceleration $\overset{\mathrm{E}\bullet}{\vec{v}}_{\mathrm{c}/w/\mathrm{E}}$ in F_{AC}, the Newton's second law, $m\overset{\mathrm{E}\bullet}{\vec{v}}_{\mathrm{c}/w/\mathrm{E}} = \vec{f}_{\mathrm{AC}}$, yields

$$m\dot{V} = -mg\sin\gamma - D + T\cos\alpha \tag{13}$$

$$mV\dot{\gamma} = -mg\cos\gamma + L + T\sin\alpha \tag{14}$$

Finally, it follows from the Euler's equation that

$$I_{yy}\ddot{\theta} = M, \tag{15}$$

where I_{yy} is the moment of inertia relative to c about the $\hat{\jmath}_{\mathrm{E}}$ axis. The longitudinal dynamics of the aircraft are given by (13), (14), and (15).

In a steady flight, $\dot{V} = 0$, the flight-path angle $\gamma = 0$, $\dot{\theta} = 0$, and thus $\alpha = \theta$. It thus follows that

$$D = T\cos\theta, \tag{16}$$

$$L = mg - T\sin\theta, \tag{17}$$

$$M = 0. \tag{18}$$

The thrust T_{trim} and elevator deflection $\delta_{\mathrm{e,trim}}$ required to maintain steady-state flight are computed by solving for T and θ that satisfy (16)-(18).

IV. Total Energy Control System

The total energy control system (TECS) is intuitively based on the idea that while thrust adds energy to an aircraft, the elevator trades kinetic and potential energy. The objective of TECS is thus the regulation of the kinetic and potential energies of the aircraft. To do so, the velocity and flight-path angle commands are first converted into total energy and energy balance commands. Modeling the aircraft as a point mass, the specific energy of the aircraft, defined as the total energy scaled by mgv, is given by

$$E = \frac{1}{mgV}\left(\frac{1}{2}mV^2 + mgh\right) = \frac{V}{2g} + \frac{h}{V}, \tag{19}$$

and the specific energy balance, defined as the difference between the kinetic energy and the potential energy scaled by mgv, is given by

$$B = \frac{1}{mgV}\left(\frac{1}{2}mV^2 - mgh\right) = \frac{V}{2g} - \frac{h}{V}. \tag{20}$$

Using (19) and (20), the velocity and altitude commands are converted into the specific energy and the specific energy balance commands.

Next, the specific energy error $\tilde{E}$ and the specific energy balance error $\tilde{B}$, defined as the difference between the desired and current specific energy and specific energy balance, respectively, are given by

$$\tilde{E} \triangleq E_{\mathrm{sp}} - E = \frac{V_{\mathrm{sp}} - V}{2g} + \left(\frac{h_{\mathrm{sp}}}{V_{\mathrm{sp}}} - \frac{h}{V}\right), \tag{21}$$

$$\tilde{B} \triangleq B_{\mathrm{sp}} - B = \frac{V_{\mathrm{sp}} - V}{2g} - \left(\frac{h_{\mathrm{sp}}}{V_{\mathrm{sp}}} - \frac{h}{V}\right). \tag{22}$$

The specific energy rate $\dot{\tilde{E}}$ and the specific energy balance error rate $\dot{\tilde{B}}$ are approximated by

$$\dot{\tilde{E}} \triangleq \dot{E}_{\mathrm{sp}} - \dot{E} = -\frac{\dot{V}}{2g} - \frac{\dot{h}}{V} \approx -\frac{k_{\mathrm{v}}(V_{\mathrm{sp}} - V)}{2g} - \frac{k_{\mathrm{h}}(h_{\mathrm{sp}} - h)}{V}, \tag{23}$$

$$\dot{\tilde{B}} \triangleq \dot{B}_{\mathrm{sp}} - \dot{B} = -\frac{\dot{V}}{2g} + \frac{\dot{h}}{V} \approx -\frac{k_{\mathrm{v}}(V_{\mathrm{sp}} - V)}{2g} + \frac{k_{\mathrm{h}}(h_{\mathrm{sp}} - h)}{V}. \tag{24}$$

Since the rate of change of velocity and altitude is not directly measured, the rate of change of velocity and altitude in (23) and (24) are approximated by the desired rate of change of velocity and altitude. Note that the positive scalars k_{v} and k_{h} determine the desired time-constant of the speed and altitude response.

The thrust and elevator deflection are finally given by

$$T = T_{\mathrm{trim}} + \Delta_{\mathrm{T}}, \tag{25}$$

$$\delta_{\mathrm{e}} = \delta_{\mathrm{e,trim}} + \Delta_{\mathrm{e}}, \tag{26}$$

where

$$\Delta_{\mathrm{T}} = k_{\mathrm{p,T}}\tilde{E} + k_{\mathrm{i,T}} \int \tilde{E} + k_{\mathrm{d,T}}\dot{\tilde{E}}, \tag{27}$$

$$\Delta_{\mathrm{e}} = k_{\mathrm{p,e}}\tilde{B} + k_{\mathrm{i,e}} \int \tilde{B} + k_{\mathrm{d,e}}\dot{\tilde{B}}, \tag{28}$$

and the thrust T_{trim} and elevator deflection $\delta_{\mathrm{e,trim}}$ required to maintain steady-state flight are computed by solving for T and θ that satisfy (16)-(18). The TECS block diagram is shown in Figure 2.

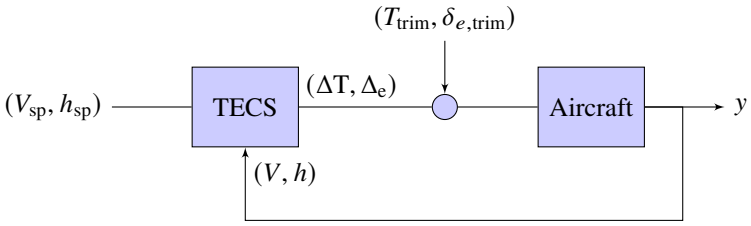

Fig. 2 Total energy control system for longitudinal aircraft dynamics control.

V. Adaptive Total Energy Control System

The adaptive TECS consists of the TECS described in the previous section with a nominal choice of gains and an adaptive PID controller based on the retrospective cost optimization. In particular, each fixed-gain controller in TECS is augmented with an adaptive controller. Thus, the thrust and elevator deflection are given by

$$T = T_{\mathrm{trim}} + \Delta_{\mathrm{T}} + u_{\mathrm{T}}, \tag{29}$$

$$\delta_{\mathrm{e}} = \delta_{\mathrm{e,trim}} + \Delta_{\mathrm{e}} + u_{\mathrm{e}}, \tag{30}$$

where, for $t \in [k\Delta t, (k+1)\Delta t)$,

$$u_{\mathrm{T}}(t) = u_{\mathrm{T},k}, \tag{31}$$

$$u_{\mathrm{e}}(t) = u_{\mathrm{e},k} \tag{32}$$

and $u_{\mathrm{T},k}$ and $u_{\mathrm{e},k}$ are computed using the retrospective cost adaptive control algorithm described in the next section. The adaptive TECS block diagram is shown in Figure 3.

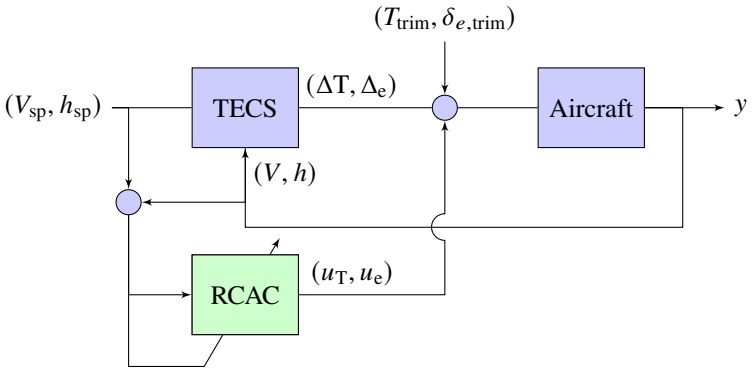

Fig. 3 Adaptive total energy control system for longitudinal aircraft dynamics control.

VI. RCAC Algorithm

This section briefly reviews the retrospective cost adaptive control (RCAC) algorithm. RCAC is a digital adaptive control technique described in detail in [16] and its extension to digital PID control is given in [17].

For all $k \geq 0$, consider the control law

$$u_k = \phi_k \theta_k, \tag{33}$$

where the regressor ϕ_k contains the measured data and the θ_k is the controller gain optimized by RCAC. For example, for a SISO PID control law,

$$\phi_k \triangleq \begin{bmatrix} z_{k-1} \\ \gamma_{k-1} \\ z_{k-1} - z_{k-2} \end{bmatrix}^{\mathrm{T}}, \quad \theta_k \triangleq \begin{bmatrix} K_{\mathrm{p},k} \\ K_{\mathrm{i},k} \\ K_{\mathrm{d},k} \end{bmatrix}. \tag{34}$$

where z_k is the error variable, $\gamma_k = \gamma_{k-1} + z_{k-1}$ is the integrator state, and $K_{\mathrm{p},k}$, $K_{\mathrm{i},k}$, and $K_{\mathrm{d},k}$ are the time-varying PID gains.

To determine the controller gains θ_k, let $\theta \in \mathbb{R}^{l_\theta}$, and consider the *retrospective performance variable* defined by

$$\hat{z}_k(\theta) \triangleq g(z_k) + \sigma(\phi_{k-1}\theta - u_{k-1}), \tag{35}$$

where $\sigma \in \mathbb{R}$. The sign of σ is the sign of the leading numerator coefficient of the transfer function from u_k to z_k. Furthermore, define the *retrospective cost function* $J_k : \mathbb{R}^{l_\theta} \to [0, \infty)$ by

$$J_k(\theta) \triangleq \sum_{i=0}^{k} \hat{z}_i(\theta)^{\mathrm{T}} R_z \hat{z}_i(\theta) + (\phi_k\theta)^{\mathrm{T}} R_u (\phi_k\theta) + (\theta - \theta_0)^{\mathrm{T}} P_0^{-1} (\theta - \theta_0), \tag{36}$$

where $\theta_0 \in \mathbb{R}^{l_\theta}$ is the initial vector of PID gains and $P_0 \in \mathbb{R}^{l_\theta \times l_\theta}$ is positive definite.

Proposition VI.1. Consider (33)–(36), where $\theta_0 \in \mathbb{R}^{l_\theta}$ and $P_0 \in \mathbb{R}^{l_\theta \times l_\theta}$ is positive definite. Furthermore, for all $k \geq 0$, denote the minimizer of J_k given by (36) by

$$\theta_{k+1} \triangleq \operatorname*{argmin}_{\theta \in \mathbb{R}^n} J_k(\theta). \tag{37}$$

Then, for all $k \geq 0$, θ_{k+1} is given by

$$\theta_{k+1} = \theta_k - \sigma P_{k+1} \phi_{k-1}^{\mathrm{T}} R_z [z_k + \sigma(\phi_{k-1}\theta_k - u_{k-1})] - P_{k+1} \phi_k^{\mathrm{T}} R_u \phi_k \theta_k, \tag{38}$$

where

$$P_{k+1} = P_k - P_k \Phi_k^{\mathrm{T}} \left(\bar{R}^{-1} + \Phi_k P_k \Phi_k^{\mathrm{T}} \right)^{-1} \Phi_k, \tag{39}$$

and

$$\Phi_k \triangleq \begin{bmatrix} \sigma \phi_{k-1} \\ \phi_k \end{bmatrix}, \quad \bar{R} \triangleq \begin{bmatrix} R_z & 0 \\ 0 & R_u \end{bmatrix}. \tag{40}$$

Proof. See [18] □

Finally, the control is given by

$$u_{k+1} = \phi_{k+1} \theta_{k+1}. \tag{41}$$

VII. Simulation Results

This section describes the experimental setup that is used to investigate the performance of the adaptive TECS and the results obtained in the simulation environment. In this paper, we use the physical properties of the A340 aircraft to simulate (16)-(18). The physical properties are given in Table 1.

Variable	Value
Mass m	255840 kg
Inertia I_{yy}	30,513,547 kg $\cdot$ m^2
Span S	60.3 m
Lift Coefficients ($C_{\mathrm{L}_0}, C_{\mathrm{L}_\alpha}, C_{\mathrm{L}_{\delta_\mathrm{e}}}$)	0.2301, 5.9598, 0.2391
Drag Coefficients ($C_{\mathrm{D}_0}, C_{\mathrm{D}_\alpha}$)	0.0172
Moment Coefficients ($C_{\mathrm{M}_0}, C_{\mathrm{M}_\alpha}, C_{\mathrm{M}_{\delta_\mathrm{e}}}$)	-0.0812, -3.1069, -0.9816

Table 1 Physical properties of the aircraft considered in this paper.

The aircraft is first assumed to be flying in a steady-state trim condition. The trim condition is obtained by numerically solving for trim thrust T_t and trim elevator δ_{e_t} that satisfy (16)-(18). Figure 4 shows the trim thrust T_{trim} and trim elevator deflection $\delta_{\mathrm{e,trim}}$ for various values of the altitude and flight speed.

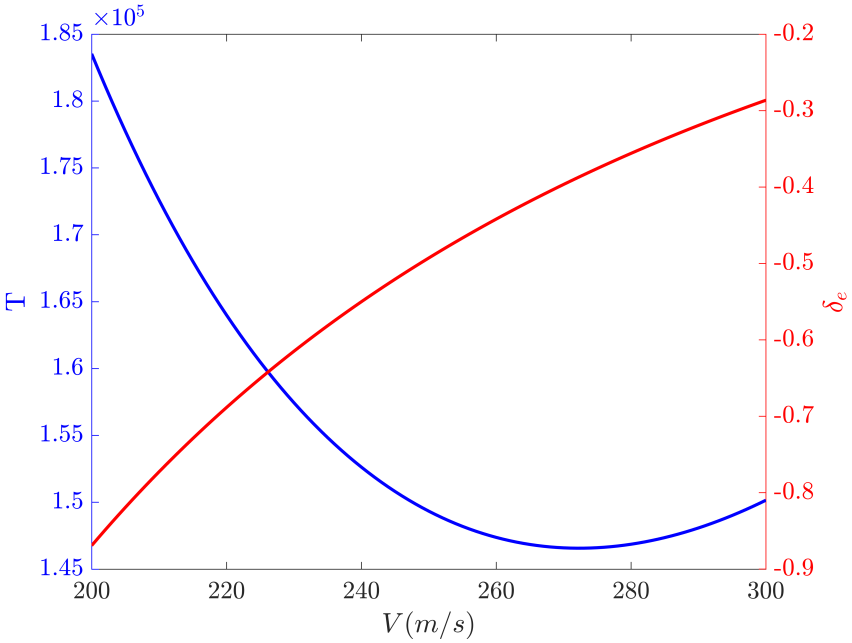

Fig. 4 Steady-state inputs T and δ_e to maintain steady-state at $h = 10,000$ m.

Next, the aircraft is commanded to follow step commands in velocity and altitude. Specifically, the aircraft is commanded to change its velocity and altitude to the various cases given in Table 2. At $t = 0$, the aircraft is assumed to be flying at steady-state with a velocity of 250 m/s at an altitude of 10,000 m. In TECS, $K_{p,T} = -3.00$, $K_{i,T} = -0.05$, $K_{d,T} = -1.00$, $K_{p,e} = 0.10$, $K_{i,e} = 0.00$, $K_{d,e} = 4.00$, $K_v = 0.22$, and $K_h = 0.10$. Figure 5 shows the closed-loop response of the aircraft with the fixed-gain TECS.

Case	(V_d, h_d)
1	(230, 9,500)
2	(240, 9,900)
3	(260, 10,100)
4	(270, 10,500)

Table 2 Desired velocity and altitude values.

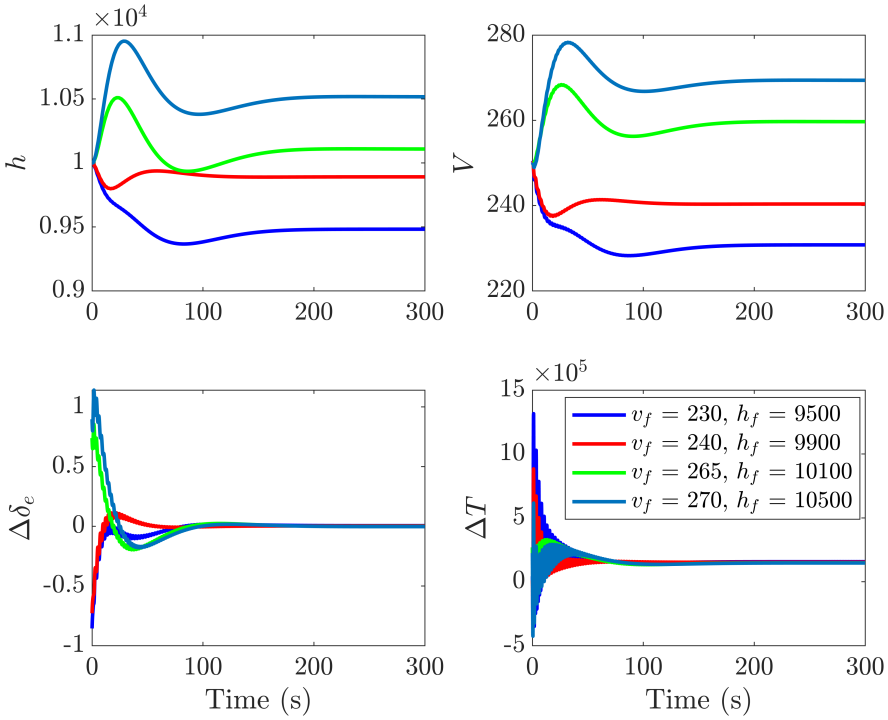

Fig. 5 Closed loop responses of the aircraft to step commands given in Table 2 with TECS.

Next, the aircraft is commanded to follow the commands given in Table 2 with the adaptive TECS controller. It is observed that the best performance improvement is obtained in the case where the thrust controller is augmented by an adaptive PD controller and the elevator deflection controller is augmented by adaptive P controller. Thus, in all of the following simulations, RCAC updates an adaptive PD and an adaptive P controller. In the adaptive thrust controller, $R_\theta = 10^3$ and $\sigma = -10$; and in the adaptive elevator-deflection controller, $R_\theta = 10^7$ and $\sigma = -10$. Figure 6 shows the closed-loop response of the aircraft with the adaptive TECS controller. Figure 7 shows the closed-loop response of the aircraft with both the TECS and the adaptive TECS controller. The solid traces are obtained with the adaptive TECS and the dashed traces are obtained with the fixed-gain TECS for the same commands. Note that the performance, in terms of settling time and overshoot, is improved as RCAC continually optimizes the controllers.

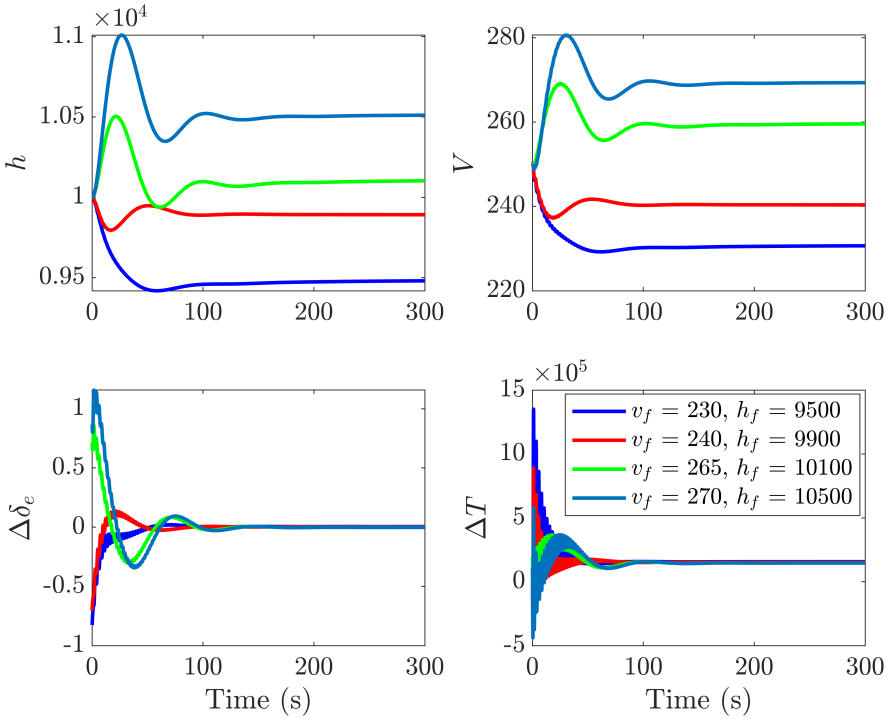

Fig. 6 Closed loop responses of the aircraft to step commands given in Table 2 with the adaptive TECS.

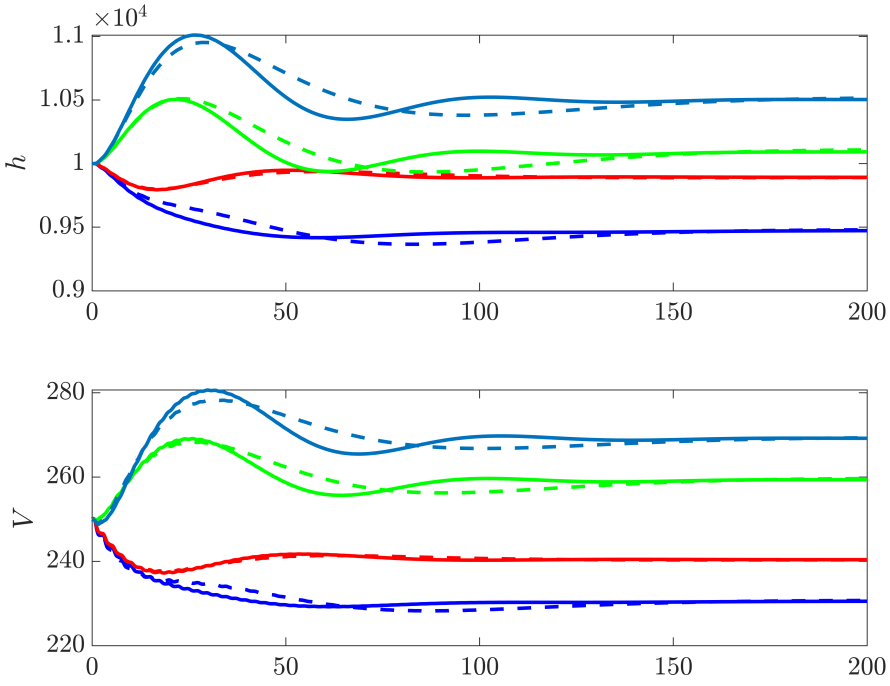

Fig. 7 Closed loop responses with the TECS (dashed lines) and the adaptive TECS (solid lines).

Next, to demonstrate the performance improvement that can be obtained by augmenting the TECS with adaptive controllers, the nominal controller gains in the adaptive TECS are scaled by a factor $\alpha > 0$. At $t = 0$, the aircraft is

assumed to be flying at steady-state with a velocity of 250 m/s at an altitude of 10,000 m, and is commanded to change its velocity to 260 m/s and its altitude to 10,100 m. Figure 8 shows the closed-loop response of the aircraft for various values of α in the case where fixed-gain TECS gains are scaled by α. Figure 9 shows the closed-loop response of the aircraft for various values of α in the case where the nominal gains in the adaptive TECS are scaled by α. Note that the adaptive controller gains compensate for the performance loss due to degraded nominal gains.

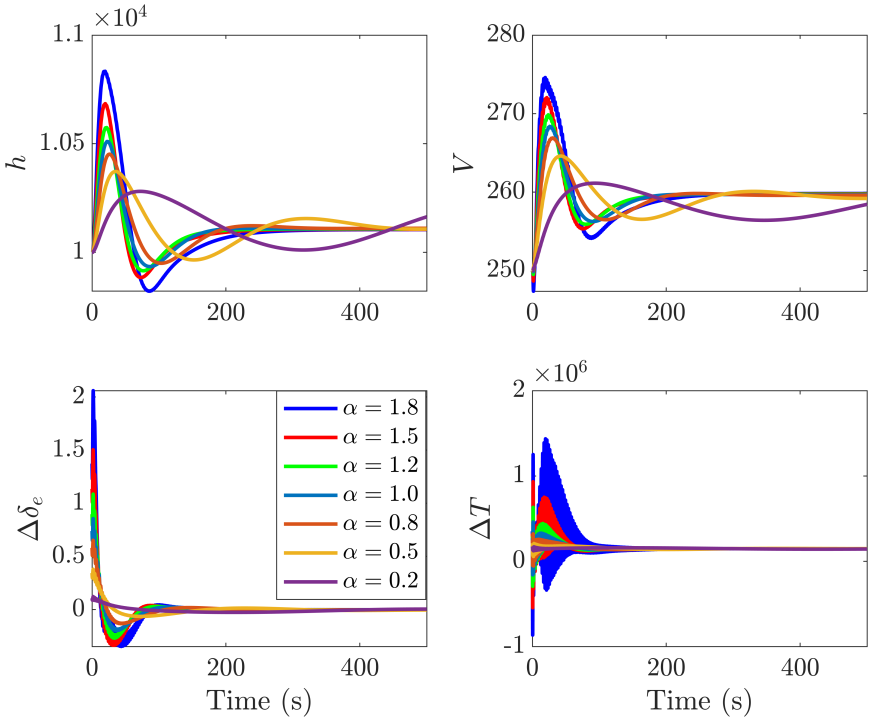

Fig. 8 Closed-loop response of the aircraft in the case where TECS gains are scaled by α.

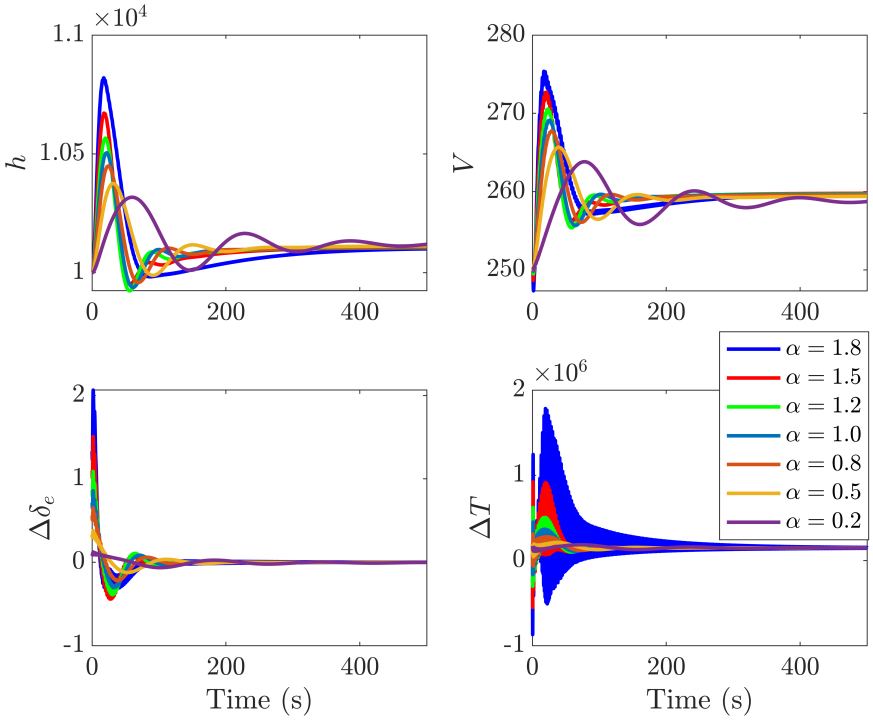

Fig. 9 Closed-loop response of the aircraft with the adaptive TECS in the case where the nominal gains are scaled by α.

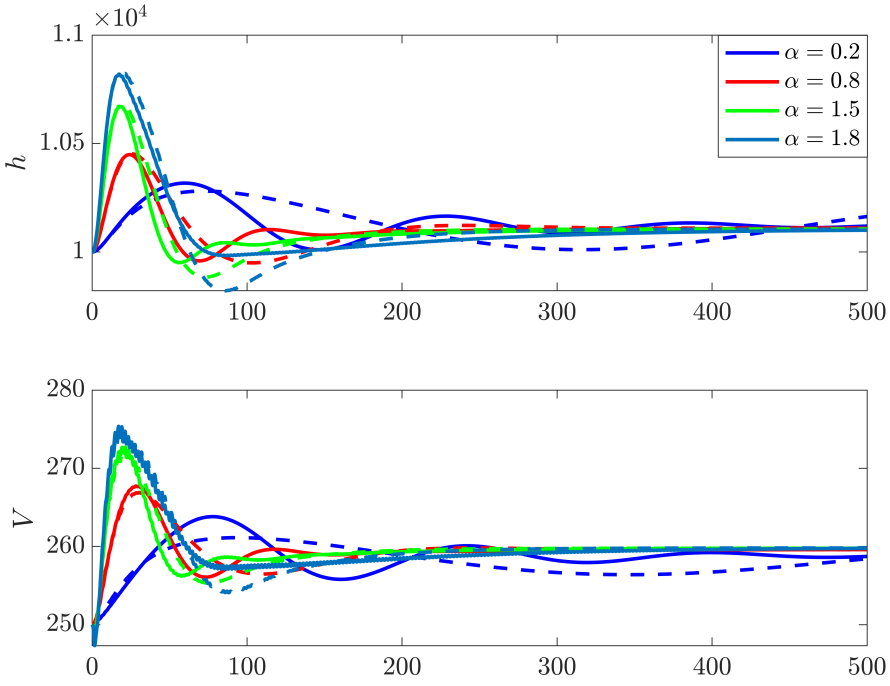

Fig. 10 TECS (dashed) and Adaptive TECS (solid) responses to degraded controller.

Finally, the effect of RCAC hyperparameters on the closed-loop performance of the aircraft is investigated. In particular, the aircraft is commanded to follow a step command in velocity and altitude for various values of R_θ and σ

which were scaled by α_θ and α_σ, respectively. Figure 11 shows the closed-loop response of the aircraft for various values of R_θ and σ. The left column shows the altitude and velocity performance for R_θ scaling, and the right column for σ scaling. Note that the closed-loop performance is only slightly affected as R_θ and σ are varied by more than two orders of magnitude. This suggests that the adaptive TECS is not very sensitive to RCAC hyperparameters.

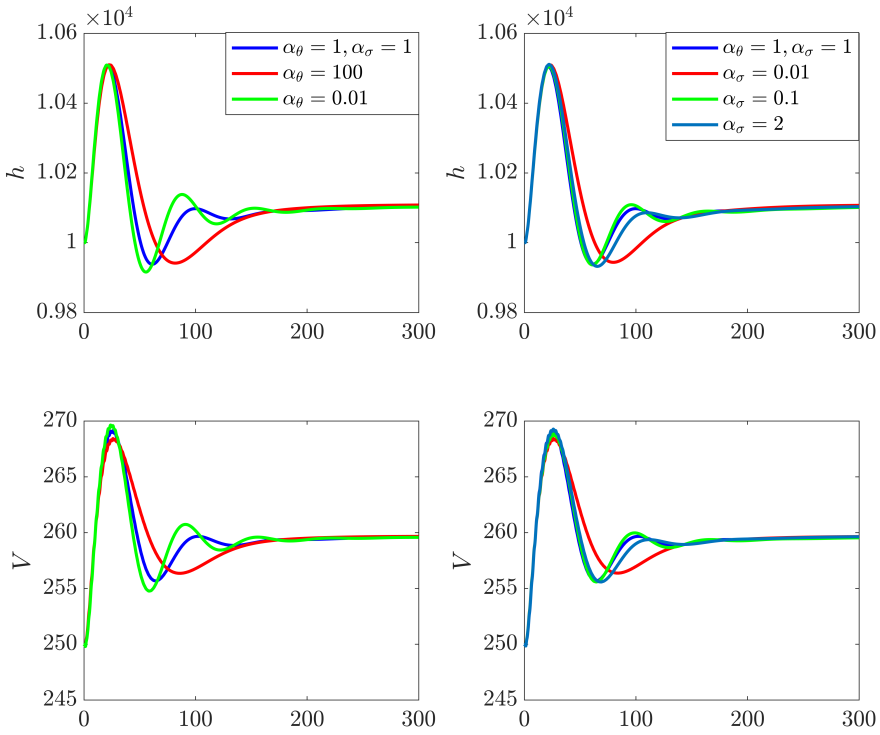

Fig. 11 Effect of RCAC hyperparameters on the closed-loop performance of the aircraft with the adaptive TECS.

VIII. Conclusions

This paper presented an adaptive total energy control system (adaptive TECS), which is constructed by augmenting the total energy control system (TECS) with adaptive controllers updated by the retrospective cost adaptive control (RCAC) algorithm. Using simulations, it was shown that the adaptive TECS improves closed-loop performance of the aircraft, in terms of settling time and overshoot. Next, it was shown that the adaptive TECS can recover the loss in performance due to degradation of the nominal TECS as the adaptive TECS continually reoptimizes the adaptive controllers. This study suggests that the adaptive TECS may have superior performance in the case where the aircraft configuration changes with time.

References

[1] R. W. Beard and T. W. McLain, *Small unmanned aircraft: Theory and practice*. Princeton university press, 2012.

[2] A. Lambregts, "Vertical flight path and speed control autopilot design using total energy principles," in *Guidance and Control Conference*, 1983, p. 2239.

[3] ——, "Integrated system design for flight and propulsion control using total energy principles," in *Aircraft design, systems and technology meeting*, 1983, p. 2561.

[4] A. Lambregts, "Functional integration of vertical flight path and speed control using energy principles," in *Proc. 1st Annu. NASA Aircraft Controls Workshop*, 1983, pp. 389–409.

[5] K. R. Bruce, "Flight test results of the total energy control system," *NASA CR-178285*, 1987.

[6] J. Brigido-González and H. Rodriguez-Cortes, "Adaptive energy based control for the longitudinal dynamics of a fixed-wing aircraft," in *2014 American Control Conference*, IEEE, 2014, pp. 715–720.

[7] L. Faleiro and A. Lambregts, "Analysis and tuning of a total energy control system control law using eigenstructure assignment," *Aerospace science and technology*, vol. 3, no. 3, pp. 127–140, 1999.

[8] C. Voth and U.-L. Ly, "Total energy control system autopilot design with constrained parameter optimization," in *1990 American Control Conference*, IEEE, 1990, pp. 1332–1337.

[9] M. E. Argyle and R. W. Beard, "Nonlinear total energy control for the longitudinal dynamics of an aircraft," in *2016 American Control Conference (ACC)*, 2016, pp. 6741–6746.

[10] A. Goel, J. A. Paredes, H. Dadhaniya, S. A. U. Islam, A. M. Salim, S. Ravela, and D. Bernstein, "Experimental implementation of an adaptive digital autopilot," in *2021 American Control Conference (ACC)*, IEEE, 2021, pp. 3737–3742.

[11] J. Spencer, J. Lee, J. A. Paredes, A. Goel, and D. Bernstein, "An adaptive pid autotuner for multicopters with experimental results," *arXiv preprint arXiv:2109.12797*, 2021.

[12] S. A. U. Islam, T. W. Nguyen, I. V. Kolmanovsky, and D. S. Bernstein, "Data-driven retrospective cost adaptive control for flight control application," 2021. arXiv: 2102.07191 [eess.SY].

[13] J. Lee, J. Spencer, J. A. Paredes, S. Ravela, D. S. Bernstein, and A. Goel, "An adaptive digital autopilot for fixed-wing aircraft with actuator faults," *arXiv preprint arXiv:2110.11390*, 2021.

[14] N. Mohseni, T. W. Nguyen, S. A. Ul Islam, I. V. Kolmanovsky, and D. S. Bernstein, "Active noise control for harmonic and broadband disturbances using rls-based model predictive control," in *2020 American Control Conference (ACC)*, 2020, pp. 1393–1398.

[15] E. Abdulhamitbilal, E. M. Jafarov, and M. Ş. Kavsaoğlu, "Matlab-simulink nonlinear modeling and simulation of aircraft longitudinal dynamics," in *Proc. of. Eurosim*, 2007.

[16] Y. Rahman, A. Xie, and D. S. Bernstein, "Retrospective Cost Adaptive Control: Pole Placement, Frequency Response, and Connections with LQG Control," *IEEE Control System Magazine*, vol. 37, pp. 28–69, Oct. 2017.

[17] M. Kamaldar, S. A. U. Islam, S. Sanjeevini, A. Goel, J. B. Hoagg, and D. S. Bernstein, "Adaptive digital PID control of first-order-lag-plus-dead-time dynamics with sensor, actuator, and feedback nonlinearities," *Advanced Control for Applications*, vol. 1, no. 1, e20, 2019.

[18] S. A. U. Islam and D. S. Bernstein, "Recursive Least Squares for Real-Time Implementation," *IEEE Control Systems Magazine*, vol. 39, no. 3, pp. 82–85, Jun. 2019.